J. Jpn. Soc. Powder Powder Metallurgy, **71** (2024) 551-555
https://doi.org/10.2497/jjspm.24-00014

Paper

Fabrication and Evaluation of the High-Temperature Bending Strength for Mo_2NiB_2-Ni Cermets

Eri TAKAHASHI[1], Akiko MORIMOTO[1], Ayumi HAYASHI[1],
Naoto SHIRAKI[1], Toshiyuki NISHIMURA[2] and Satofumi MARUYAMA[1]*

[1]Department of Mechanical Engineering, Faculty of Science and Engineering, Tokyo City University,
1-28-1 Tamazutsumi Setagaya-ku, Tokyo 158-8557, Japan.
[2]National Institute for Materials Science, 1-2-1 Sengen, Tsukuba 305-0047 Japan.

Received February 29, 2024; Revised June 17, 2024; Accepted June 17, 2024; J-STAGE Advance Published date: June 28, 2024

ABSTRACT

Mo_2NiB_2-Ni cermets, a type of boride-based cermet, exhibit attractive mechanical properties such as high hardness and good wear resistance. However, the mechanical properties of these cermets have predominantly been evaluated at room temperature. In this study, three-point bending tests were conducted at high temperatures to investigate the mechanical properties and fractography of Mo_2NiB_2-Ni cermets. A ternary Mo_2NiB_2-Ni cermet was prepared using a calcination process to synthesize Mo_2NiB_2 before sintering. The calcination process resulted in finer and more uniform Mo_2NiB_2 particles, enhancing the microstructure. Consequently, hardness and transverse rupture strength (TRS) were improved. Three-point bending strengths were measured for samples measuring 4.0 × 3.0 × 24 mm at temperatures up to 800°C in an argon environment, using silicon carbide jigs with a 16 mm span. The results indicated that TRS remained approximately constant at about 1.6 GPa up to 500°C but decreased sharply above 600°C, reaching about 0.12 GPa at 800°C. This decrease was attributed to the softening of the nickel binder phase, which adversely affected the TRS.

KEY WORDS

boride, cermets, mechanical properties

1 Introduction

Transition metal borides are known for their hardness, chemical stability, and high melting points[1-4]. Despite their inherent brittleness, K. Takagi pioneered the development of these materials into cermets—composite materials composed of boride ceramics and metals[1]. Metal boride cermets are viewed as viable alternatives to WC-Co cemented carbides traditionally used in the manufacture of cutting tools and wear-resistant materials[5,6]. Boride-based cermets such as Mo_2NiB_2, Mo_2FeB_2, and WCoB are produced through a powder metallurgy process known as reaction boronizing sintering (RBS), introduced by K. Takagi[7-9]. This method involves liquid phase sintering and the in-situ formation of ternary borides within a metal matrix, achieved through the reaction of binary borides with metallic elements during a one-shot sintering process[10]. Mo_2NiB_2–Ni based cermets have garnered attention due to their notable mechanical properties and corrosion resistance[11].

Recent studies have explored the electronic structures of orthorhombic (ort-) Mo_2NiB_2 and tetragonal (tet-) Mo_2NiB_2 phases through first-principles calculations. Li J. et al. examined the electronic structure and elastic properties of the Mo_2NiB_2 phase, including the effects of vanadium (V) doping[12]. Similarly, Y. Jian et al. investigated the phase stability and mechanical properties of the tet- and ort- Mo_2NiB_2 ternary phases[13]. Investigations into the substitution of chromium (Cr) or vanadium (V) in Mo_2NiB_2, which influence the crystal structure and mechanical properties, were conducted by J. Watanabe et al. through experiments and first-principles calculations[14]. Additionally, the Crystal Orbital Hamilton Population (COHP)[15] analysis has been used to assess the superior mechanical properties of tetragonal Cr or V substituted Mo_2NiB_2, attributing the enhancement to strong bonding between Mo-(Cr or V) and (Cr or V)-B atoms[16].

Despite these advancements, few studies have addressed the high-temperature mechanical properties of Mo_2NiB_2-Ni cermets. M. Komai has reported on the temperature dependence of transverse rupture strength (TRS)[17], and L. Zhang has examined the high-temperature compressive properties and tribological behavior of Mo_2NiB_2-Ni cermets[18]. Nonetheless, the fracture behavior of Mo_2NiB_2-Ni cermets at elevated temperatures remains largely unexplored. This gap in the research highlights the need for

* Corresponding author, E-mail: smaruyam@tcu.ac.jp
** The contents of this article had been presented at JSPMIC2023.

detailed high-temperature bending tests and subsequent analyses of fracture surfaces. Consequently, this study was initiated to investigate the fracture behavior of Mo_2NiB_2-Ni cermets under high-temperature conditions.

2 Experiment

Ternary Mo_2NiB_2-Ni cermet was fabricated using two approaches: the conventional RBS and an innovative method involving a calcination process prior to sintering. According to H. Wu, calcination of Mo_2FeB_2 powder enhances the homogeneity of the microstructure and the mechanical properties of Mo_2FeB_2-based cermets[19].

The Mo_2NiB_2 pre-sintered powder was produced through a solid-state reaction. MoB and Ni powders were measured in a molar ratio of 2:1 and mixed in a pot mill with acetone as the solvent at a rotation speed of 200 rpm for 24 h. The mixture was then thoroughly dried to obtain a homogeneous mixed powder, which was subsequently placed in a graphite crucible and calcinated at 1,000°C for 5 h under vacuum conditions.

After calcination, the mixture was ground using a Si_3N_4 mortar and pestle, and then mixed with additional Ni powder. The proportions of Mo_2NiB_2 calcinated powder to Ni are detailed in Table 1. For comparative purposes, samples using the conventional RBS method were also prepared, with the mixing ratios also presented in Table 1. Samples from the conventional RBS method are denoted as "RBS," while those from the calcination process are labeled "Pre." The powders, along with 3 wt.% paraffin, were milled using a planetary ball mill at 200 rpm for 3 h in acetone, dried, pressed, and sintered on a graphite plate in an electric furnace under a vacuum of about 10 Pa. Fig. 1 illustrates the temperature profile for the sintering process, which involved holding the samples at 180°C and 300°C for 30 min each to remove paraffin, at 1,000°C for 60 min to facilitate reaction and deoxidation, and finally at 1,250°C for 60 min.

Table 1 Mass fractions of starting materials for Mo_2NiB_2-Ni cermets fabricated by the via-calcination process and RBS process.

Sample name	MoB	Mo_2NiB_2	Ni
RBS	62.8	-	37.2
Pre	-	80	20

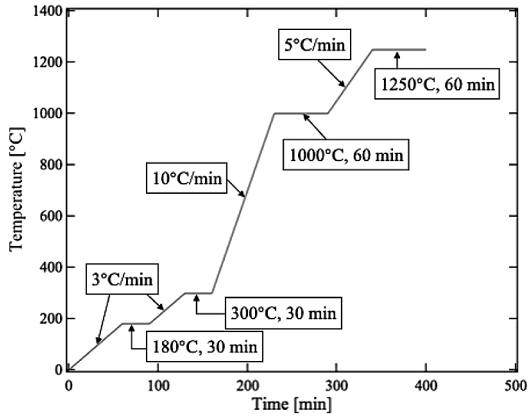

Fig. 1 Temperature profile for the sintering process.

Characterization of the samples included X-ray diffraction (XRD) measurements and Rietveld refinements, along with scanning electron microscopy (SEM) for microstructural analysis. Hardness was evaluated using the Rockwell A-scale, and TRS tests at room temperature were performed on 4 mm × 8 mm × 25 mm test bars using three-point loading with a 20 mm span.

High-temperature bending tests were conducted on 3 mm × 4 mm × 25 mm test bars. These tests measured three-point bending strength at temperatures up to 800°C in an argon environment, with a crosshead speed of 0.5 mm/min and a 16 mm span, using SiC jigs.

3 Result and discussion

3.1 Effect of calcination process and room temperature mechanical properties

XRD patterns of samples prepared by RBS and the calcination process (Pre) are displayed in Fig. 2. Both samples showed the presence of Mo_2NiB_2 and Ni phases. The lattice constants of Ni calculated from Rietveld analysis, shown in Table 2, indicate that the Ni phase in both samples exhibited an increased lattice constant compared to pure Ni (a = 0.35269 nm)[20]. This increase is attributed to the formation of a solid solution with Mo and B from the Mo_2NiB_2 phase.

SEM images of the polished surfaces of the samples are shown in Fig. 3. The bright phase represents Mo_2NiB_2, the gray phase indicates Ni, and the black areas are pores. The hard phase particles in the RBS samples were coarse and varied in size, whereas those in the Pre samples were fine and uniform. Porosity, as calculated

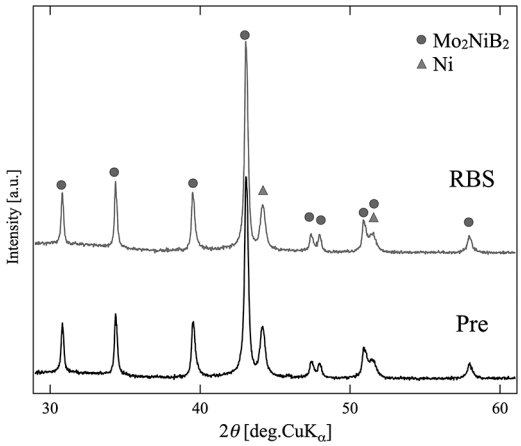

Fig. 2 XRD patterns of Mo_2NiB_2-Ni cermets for RBS and Pre samples.

Table 2 Lattice parameters of the Ni phase in Mo_2NiB_2-Ni cermets.

Sample name	RBS	Pre	Ni (ref)[20]
Lattice constant (nm)	0.35545(2)	0.35530(2)	0.35269

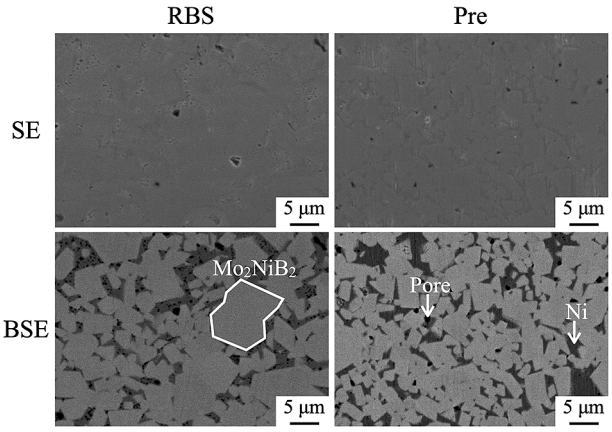

Fig. 3 Secondary electron (SE) and backscattered electron (BSE) images of the polished surfaces of Mo_2NiB_2-Ni samples.

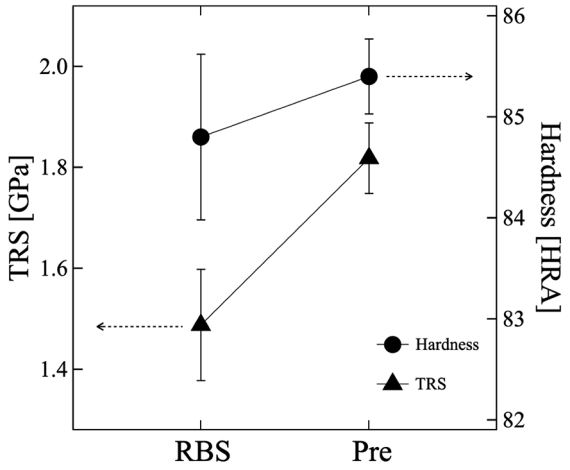

Fig. 4 Impact of sintering processes on HRA hardness and TRS.

using ImageJ software, was approximately 1.8% for the RBS samples and 0.6% for the Pre samples, demonstrating that the calcination process effectively reduced porosity. The Pre method, which separates Mo_2NiB_2 phase formation from the sintering process, employed ball milling to pulverize the calcinated Mo_2NiB_2 powder and uniformly mix it with Ni powder. This ensured a homogeneous microstructure with minimal abnormal grain growth during the subsequent liquid phase sintering.

TRS and Rockwell Hardness results for the RBS and Pre samples are presented in Fig. 4. The application of the calcination process improved both hardness and TRS while reducing variability. Fig. 5 illustrates the fracture origins after TRS tests at room temperature. In the RBS samples (Fig. 5 (a)), coarse pores were observed at the fracture origins, which are known to reduce TRS due to stress concentration[21]. Conversely, the fracture surfaces of the Pre samples (Fig. 5 (b)) showed no coarse pores at the fracture origins, correlating with higher TRS values. The presence of coarse pores in RBS samples can be attributed to the agglomeration of the Mo_2NiB_2 phase or uneven sintering progress, typical of reaction sintering processes. Thus, the Pre samples, which exhibited no

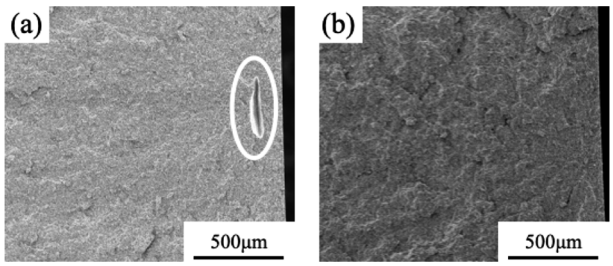

Fig. 5 SE images of fracture origins after room temperature bending tests.

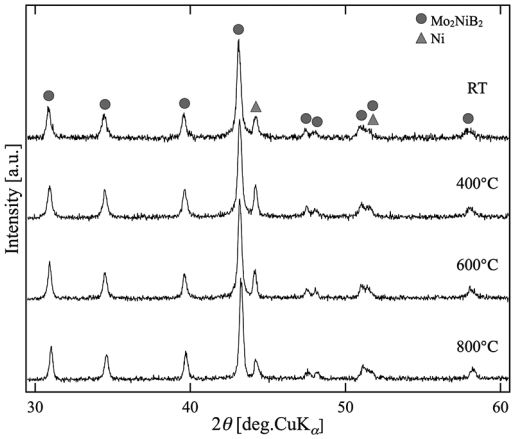

Fig. 6 XRD patterns of Mo_2NiB_2-Ni cermets post high-temperature bending tests.

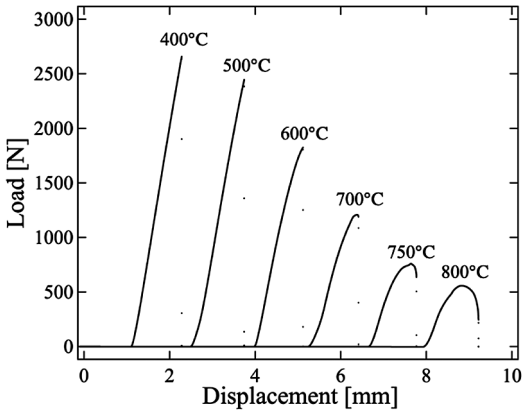

Fig. 7 Load-displacement curves from high-temperature bending tests.

coarse fracture origins, demonstrated improved TRS compared to their RBS counterparts.

3.2 High-temperature mechanical properties

High-temperature three-point bending tests were conducted on the Pre samples at various temperatures, including twice at room temperature, 400°C, 500°C, 600°C, and 700°C, and once at 750°C and 800°C. The XRD patterns from the samples after testing at 400°C, 600°C, and 800°C (shown in Fig. 6) confirmed that no phase changes occurred due to the high-temperature bending tests.

Load-displacement curves, depicted in Fig. 7, indicate that Mo_2NiB_2-Ni samples exhibited elastic deformation up to 500°C. Above this temperature, the deformation mode shifted to plastic,

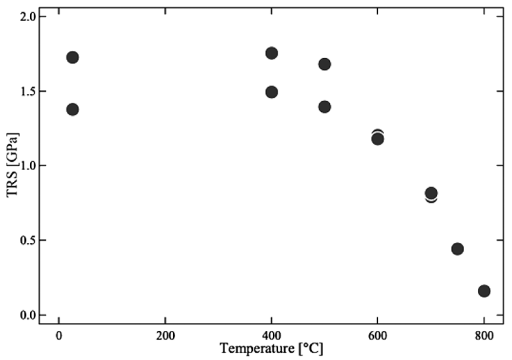

Fig. 8 TRS temperature dependence for Mo_2NiB_2-Ni samples.

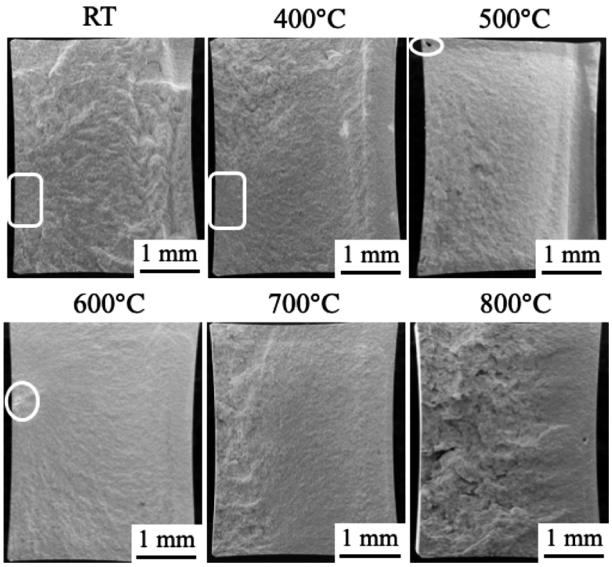

Fig. 9 Macroscopic view of fracture surfaces following the high-temperature three-point bending test. Circles highlight the fracture origins.

with a noticeable reduction in breaking loads compared to maximum loads beginning at 700°C, likely due to the softening of the samples.

Fig. 8 presents the temperature dependence of the TRS for Mo_2NiB_2-Ni samples. TRS values remained stable at approximately 1.6 GPa from room temperature up to 500°C. However, above 600°C, TRS values decreased sharply, dropping from around 1.2 GPa to 0.16 GPa as the temperature increased.

The macroscopic examination of the fracture surfaces after testing is illustrated in Fig. 9. The left side of each fracture surface corresponds to the tensile side. SEM analysis of the fracture surfaces at 500°C revealed the presence of coarse pores, identified as fracture origins. Above 600°C, the fracture surfaces appeared coarser, and distinct fracture origins became unidentifiable above 700°C. This change correlates with the softening of the Ni phase above 600°C, leading to a rougher fracture surface around the fracture origin due to altered crack propagation dynamics and a reduction in crack propagation speed.

Detailed SEM observations of the fracture surfaces are provided in Fig. 10. Up to 500°C, intragranular fracture was predominantly

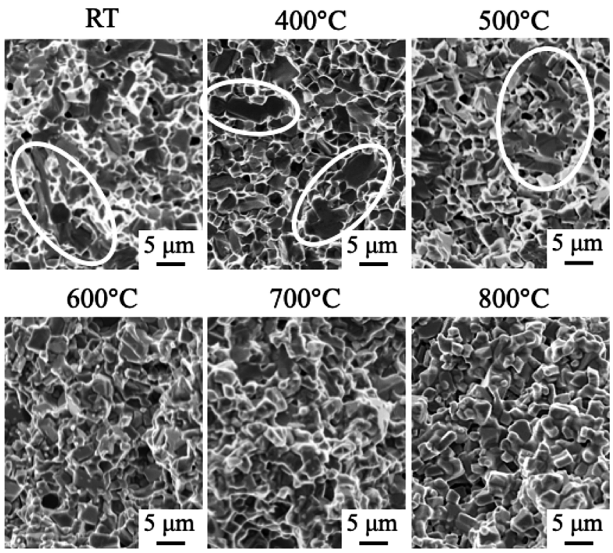

Fig. 10 Detailed SE images of fracture surfaces after high-temperature bending tests. Circles highlight intragranular fractures.

observed. However, above 600°C, the fracture mode transitioned primarily to intergranular fracture, with noticeably coarser fracture surfaces. It is concluded that the resistance to deformation and the intergranular bonding strength decreased concurrently with Ni softening. Consequently, the prevalence of intergranular fractures increased, and the roughness of the fracture surfaces also intensified.

4 Conclusion

In this study, Mo_2NiB_2-Ni cermets were synthesized using a calcination process prior to sintering to refine the hard phase particles and investigate their mechanical properties at elevated temperatures.

(1) The introduction of the calcination process led to the synthesis of finer and more uniform Mo_2NiB_2 particles. This occurred because the Mo_2NiB_2 was synthesized in advance, allowing for a uniformly generated liquid phase throughout the material during sintering, which facilitated uniform grain growth and densification.

(2) Samples produced using the calcination process exhibited higher TRS and hardness compared to those produced via the conventional RBS method. These improvements can be attributed to the suppression of vacancy generation and the creation of finer, more homogeneous hard phase particles.

(3) The TRS values remained constant from room temperature up to 500°C but experienced a sharp decline above 600°C. This decline is likely due to the softening of the Ni phase, which reduced deformation resistance and increased the prevalence of intergranular fractures on the fracture surfaces.

(4) The high-temperature bending behavior of the Mo_2NiB_2-Ni cermet is primarily influenced by the thermal response of the Ni binder phase, demonstrating a critical dependency on the Ni phase behavior at high temperatures.

Acknowledgment

This work was partially supported by TCU Prioritized Studies.

References

1) K. Takagi: J. Solid State Chem., **179** (2006) 2809-2818.
2) B. R. Golla, A. Mukhopadhyay, B. Basu, S. K. Thimmappa: Prog. Mater. Sci., **111** (2020) 100651.
3) T. Jüngling, L. S. Sigl, R. Oberacker, F. Thümmler, K. A. Schwetz: Int. J. Refract. Met. H., **12** (1993-1994) 71-88.
4) B. A. Cook, J. L. Harringa, T. L. Lewis, A. M. Russell: Scripta Mater., **42** (2000) 597-602.
5) G. Suskin, G. I. Chepovetsky: J. Mater. Eng., **5** (1996) 396-398.
6) J. García, V. Collado Ciprés, A. Blomqvist, B. Kaplan: Int. J. Refract. Metals Hard Mater., **80** (2019) 40-68.
7) M. Komai, Y. Yamasaki, K. Takagi: Solid State Phenom., **25-26** (1992) 531-538.
8) T. Ide, K. Nakano, K. Takagi: J. Jpn. Soc. Powder Powder Metall., **34** (1987) 302-308.
9) M. Komai, Y. Isobe, K. Takagi: J. Jpn. Soc. Powder Powder Metall., **40** (1993) 38-43.
10) K. Takagi: J. Jpn. Soc. Powder Powder Metall., **45** (1998) 507-514.
11) K. Iwanaga, K. Hirata, Y. Yamasaki, M. Inoue, K. Takagi: J. Jpn. Soc. Powder Powder Metall., **53** (2006) 214-220.
12) J. Li, X. Li, H. Gao, D. Peng: Mod. Phys. Lett. B, **32** (2018) 1850065.
13) Y. Jian, X. Huang, X. Liu, J. Xing: Results Phys., **15** (2019) 102698.
14) J. Watanabe, T. Ota, S. Maruyama: Solid State Sci., **108** (2020) 106373.
15) R. Dronskowski, P. E. Blöchl: J. Phys. Chem., **97** (1993) 8617-8624.
16) J. Watanabe, R. Koyama, S. Maruyama: J. Jpn. Soc. Powder Powder Metall., **68** (2021) 278-285.
17) M. Komai, K. Takagi: Mater. Jpn., **33** (1994) 1514-1523.
18) L. Zhang, Z. F. Huang, Y. P. Shen, K. M. Li, Z. Cao, Y. X. Jian, Z. J. Ren: Cera. Int., **45** (2019) 18413-18421.
19) H. Wu, Y. Zheng, Z. Han, X. Xu, X. Lu, W. Zhou: Mat. Charact., **182** (2021) 111557.
20) R. P. Anantatmula, D. Bruce Masson: Metall. Trans., **5** (1974) 605-613.
21) H. Suzuki, H. Matsubara, T. Saitoh: J. Japan Inst. Metals, **48** (1984) 1011-1016.